

Resource overheads and attainable rates for trapped-ion lattice surgery

Hudson Leone, Thinh Le, and S. Srikara

Center for Quantum Software and Information – University of Technology Sydney

Simon Devitt^{*}

Center for Quantum Software and Information – University of Technology Sydney and
InstituteQ, Aalto University, 02150 Espoo, Finland.

(Dated: June 28, 2024)

We present estimates for the number of ions needed to implement fault-tolerant lattice surgery between spatially separated trapped-ion surface codes. Additionally, we determine attainable lattice surgery rates given a number of dedicated “communication ions” per logical qubit. Because our analysis depends heavily on the rate that syndrome extraction cycles take place, we survey the state-of-the art and propose three possible cycle times between 10 and 1000 μ s that we could reasonably see realised provided certain technological milestones are met. Consequently, our numerical results indicate that hundreds of resource ions will be needed for lattice surgery in the slowest case, while close to a hundred thousand will be needed in the fastest case. The main factor contributing to these prohibitive estimates is the limited rate that ions can be coupled across traps. Our results therefore indicate an urgent need for improved optical coupling in order for trapped-ion quantum computers to scale.

I. INTRODUCTION

Trapped ions are among the best studied and most technologically mature type of qubits to date; Their long coherence times and high-fidelity gates alone justify them as a candidate qubit for scalable quantum computing [1]. How a quantum computer is scaled will depend on its underlying architecture. Broadly speaking, an architecture may be *monolithic* [2] or *modular* [3]. A monolithic architecture is scaled by increasing the size of the chip, while a modular architecture is scaled by increasing the number of chips. Physical constraints and routing overheads generally cap the number of qubits that a monolithic architecture can reasonably support, which makes modularity something of an informal requirement when scaling quantum computers. Another requirement for scalability is error correction [4]. Industrial applications for quantum computing require programs to run for hours or even days. This is considerably longer than the coherence times of trapped ions, which means that computational qubits must be encoded and periodically corrected.

Based on these considerations, we expect that scalable quantum computers will be both *modular* and *error corrected*. One obvious disadvantage of the modular architecture is that two-qubit operations are *not intrinsically possible* between qubits that live in separate modules. Instead, some amount of entanglement has to be shared between modules as a resource for *state* or *gate teleportation* [5]. This process is complicated by the fact that entanglement distribution is *probabilistic* and *noisy*. To say that distribution is probabilistic means there is a significant chance of failure when attempting to entangle two physical qubits. For inter-modular two qubit operations to be reliable, this means that a large number of

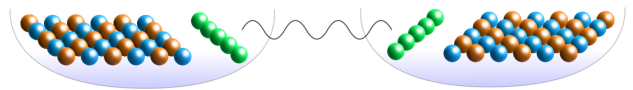


FIG. 1. A collection of trapped ions in two separate Elementary Logical Units (ELUs). Some of the ions in each trap are used to encode a logical surface code qubit while other *communication ions* collect and refine entanglement to be used for a two-qubit *lattice surgery* operation.

communication qubits will be required as an overhead to ensure that enough entanglement is collected. On the other hand, to say that distribution is noisy means that errors are inadvertently introduced into the entangled states which must be corrected before any teleportation can take place. This correction is done through *entanglement purification* [6] which non-deterministically reduces a large ensemble of weakly entangled pairs into a smaller ensemble of strongly entangled pairs.

In this paper, we conduct resource analysis on the number of ions needed to implement *reliable* two qubit operations between logically encoded qubits in different modules at different speeds. Specifically, we limit our attention to the *lattice-surgery* operation between *surface-code* encoded qubits (See Fig. 1 for a simplified schematic). This analysis is significantly influenced by the speed at which lattice surgery can be performed. Faster operations are desirable of course, but myriad factors limit the attainable rate. To ground our analysis, we survey the state-of-the-art in trapped-ion technologies and synthesise this information to propose *three possible surgery times* together with a rubric of technological milestones that are necessary to achieve each one. Additionally, we determine the attainable rates for lattice surgery operations given a fixed number of ions.

* Simon.Devitt@uts.edu.au

II. BACKGROUND

A. Surface code and lattice surgery

An $[[n, k, d]]$ stabilizer code is a quantum error correcting code that uses n physical qubits called *data qubits* to encode k logical qubits with a code distance d . The code is specified (non-uniquely) by $n - k$ independent stabilizer generators that define the set of valid codewords. Each stabilizer generator is an observable that is implemented by measuring an ancilla qubit (also called a *measure* or *syndrome* qubit) that has been coupled to a number of data qubits. Assuming each stabilizer generator has its own measure qubit, the total number of physical qubits needed for an $[[n, k, d]]$ stabilizer code is $n_{\text{phys}} = n + (n - k) = 2n - k$. A *stabilizer code cycle* or *syndrome extraction cycle* is a measurement of all $n - k$ stabilizers (typically implemented in parallel) which results in a collection of measurement outcomes called *syndromes* ($s \in \{+1, -1\}^{n-k}$). When syndrome extraction cycles are repeated multiple times, changes in syndromes can be used to infer the most likely physical errors that have occurred in the code.

The surface code [7] is a popular choice of stabilizer code because of its high error tolerance (between 0.1% and 1% for unbiased noise [8] and up to 43.7% for biased noise [9]) and because it can be implemented using only nearest-neighbor qubit interactions. Crucially, (and unlike the majority of codes) it is also known how to perform universal quantum computation on surface code encoded qubits [10]. In its original implementation, the surface code is a $[[d^2 + (d - 1)^2, 1, d]]$ stabilizer code. In this paper however, every mention of the surface code will refer to a similar (but slightly more efficient) variant called the *rotated surface code* which has the parameters $[[d^2, 1, d]]$.

One of the necessary conditions for universality is the existence of an *entangling gate*. Several options exist for implementing two-qubit entangling gates between surface code qubits, though we limit our consideration to just two. A *transversal gate* is performed by coupling every physical qubit in one code to a counterpart in an adjacent code. These transversal operations are challenging to implement in two-dimensional architectures due to the numerous *non-local* interactions required [11]. An easier alternative is *lattice surgery* which, unlike transversal gates, can be implemented with only nearest neighbor interactions [12]. In brief, lattice surgery is executed by performing a syndrome extraction over two code patches as if they were one elongated patch. The disadvantage of lattice surgery is that, unlike a transversal gate, it requires measurements on a subset of the physical qubits that can introduce new, undetected errors into the ensemble. To correct for this, it is necessary to perform at least d rounds of lattice surgery to build confidence that the operation was done correctly. This makes lattice surgery slow compared to the transversal gate but is still the favored option on account of its feasibility.

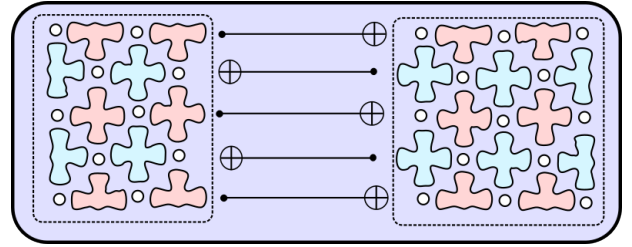


FIG. 2. An illustration of the lattice surgery operation between two surface code encoded qubits. The white circles represent data qubits which work together to encode the logical qubits in either box. The floral tiles represent *syndrome extraction circuits* which are executed in parallel to obtain information about errors that may have occurred on the data qubits. During a lattice surgery operation, two code patches undergo a syndrome extraction cycle together as if they were one elongated patch. For codes of distance D , lattice surgery requires D entangled pairs along the seam to implement the D CNOTs depicted. The effect of this operation is an XX parity check between the two encoded qubits which, with single qubit gates, is sufficient for universal quantum computing.

An important, though unrelated, fact is that transversal gates and lattice surgery can both be performed on surface codes that are not directly adjacent in space by using shared entanglement. Specifically, maximally entangled qubit pairs can be used to teleport the required two-qubit gates in either case. For surface codes of distance d , transversal gates require a total of d^2 pairs since each qubit in a $d \times d$ lattice must be matched up with its counterpart in the other lattice. Coincidentally, lattice surgery also requires d^2 pairs since d pairs are needed for each of the d rounds that are necessary to account for measurement errors. Although these two operations require the same total amount of entanglement, the *rate* of required entanglement is much smaller for lattice surgery since only d pairs are required at each time-step.

It was previously thought that the *infidelities* of the entangled pairs used in lattice surgery must at least match the error threshold of the code, however recent work by Ramette et. al. indicates that pairs can tolerate an order of magnitude more error than expected [13]. The reason for this robustness stems from the fact that entangled pairs contribute errors along a single spatial dimension of the code during lattice surgery which limits the number of ways in which errors can form paths in the code.

B. Trapped-ion architectures

Monroe et. al. [14] were among the first to perform a systematic study of a modular trapped-ion architecture, and some of our our terminology follows from their work. The modular trapped-ion computer is a collection of Elementary Logic Units (ELUs) which serve as local processors and or memory banks. In the Monroe framework, each ELU is a linear Coulomb crystal con-

taining an identical quantity of ions. Some of these are *communication ions* which are coupled to photonic interconnects and can be used to create entangled pairs between ELUs. Still another fraction of the ions are may be used for sympathetic cooling, which is when one ion is brought in proximity to another to absorb some of its vibrational energy.

An attractive advantage of the linear crystal is that it is *all-to-all* connected: No rearrangement is needed to implement a two-qubit gate between any pair of ions, though there's an effective limit to the crystal's length. Monroe et. al. believed this limit to be around 100 ions which, ten years later, seems to be a well justified estimate since the longest linear crystal today is around 30 computational qubits [15]. Further corroborating evidence for this limit is discussed in greater detail by Murali et. al. [16]. On the other hand, Ratcliffe et. al. [17] propose a *micro-trap* based architecture with all-to-all connectivity which they claim can be scaled beyond a linear trap. This is accomplished with a *non-adiabatic gate* which, at the cost of higher power, circumvents the need to use conventional side-band resolving gates which are slow and more susceptible to vibrational noise. A two dimensional extention to the microtrap architecture has also been studied in some detail [18].

In practice, we do not need to restrict ourselves by limiting the ELU to a single linear crystal. One possible workaround for further scaling is to have multiple crystals "chained together" in the same ELU to form a *segmented linear trap* [19]. The crystals in this chain can be separated, combined, and rotated to move a qubit in one crystal to any other crystal in the trap. Though the segmented linear trap has a larger qubit capacity, it lacks the all-to-all connectivity of a single crystal – meaning that some amount of physical routing is required for general computation. On average, the number of swap operations needed to move quantum information from one end of the chain to the other scales linearly with the number of modules and the number of qubits per segment. Monroe et. al. believe more optimistically that a maximum of 1000 ions should be possible in an segmented linear trap [14].

A still more general option for an ELU architecture is a Quantum Charged Coupling Device (QCCD) [19] [20]. This is a two-dimensional configuration of ion chains which may be routed along a fixed network of corridors and junctions. Theoretically, QCCD architectures are monolithic, well connected, and faster than segmented linear traps, though they are difficult to fabricate and currently limited to around ten qubits. For a survey on the technical challenges of scaling QCCDs, see Murali et. al. [16]. True two and three dimensional ion crystals (also called Wigner crystals) may also be possible to engineer in the future on the scale of hundreds or perhaps even thousands of ions [21] [22].

C. Trapped-ion surface code implementations

Specialised architectures for *quantum error correction* will likely be easier to realise in the near term since error correction is predictable, repetitive, and often nearest neighbor (as is the case for the surface code). Though an experimental demonstration of a trapped-ion surface code has yet to be realised, there is nevertheless a growing body of theoretical work around this objective. LeBlond et. al. presented software for compiling surface code operations to trapped-ion hardware [23]. Trout et. al. conducted extensive simulations of a distance 3 surface code implemented in a trapped-ion linear array [24], and reported a pseudothreshold of 3×10^{-3} with syndrome cycle times ranging from around 3 to 8 milliseconds. Similarly, Li et. al. studied a surface code modeled on a segmented linear trap [25]. For segment lengths of around 15 qubits, they report an error tolerance of 0.12% but say nothing about syndrome extraction times. Lekitsch et. al. [26] present a proof-of-concept for a monolithic surface code architecture that closely resembles a QCCD. A crucial difference however is that the Lekitsch architecture relies on *global fields* for a majority of the operations instead of individual lasers, which they argue is more feasible for monolithic scaling since it circumvents the need to align many optical elements with high precision. Their proposed cycle times are around $300\mu s$.

III. ESTIMATING SURFACE CODE CYCLE TIMES

The rate we are able to do lattice surgery is upper bounded by the rate at which *syndrome extraction cycles* can be performed. Some care is therefore required to establish reasonable estimates for the attainable cycle times in trapped-ion systems. The required time will depend not only on the specific architecture, but also various factors such as the speeds of single and two-qubit gates, measurements, ion-shuttling and cooling. We consider each of these factors in the following subsections and conclude our review by establishing three *cycle time paradigms* we expect are feasible provided that specific technological milestones are met.

A. Trapped-ion gates

The review of Bruzewicz et. al. presents a thorough comparison of single and two qubit trapped-ion gate times [27]. Typical single qubit gates with fidelities greater than surface code threshold are reported between $2\mu s$ and $12\mu s$, though lower fidelity operations have been demonstrated on the order of nanoseconds. Two qubit gates are generally slower and lower fidelity. Typical two-qubit gates with fidelities *close* to a desired operational rate of 0.1% error threshold are clocked between $1.6\mu s$ and $30\mu s$. It is not unreasonable to assume therefore

that the time it takes to implement the gates in a surface code cycle is around $10\mu\text{s}$.

B. Trapped-ion measurements

Single-qubit trapped-ion measurements are commonly implemented via *state-dependent fluorescence*. In this method, laser light is directed at an ion which exclusively couples the $|1\rangle$ state to a ‘cycling transition’ that scatters numerous easily detectable photons. Likewise, the absence of photons indicates a measurement of the $|0\rangle$ state [27]. Although fluorescence measurements are relatively fast (on the order of $10\mu\text{s}$ [28] [29]) and high fidelity, the scattered photons (both from the laser and from the irradiated ion) are likely to decohere nearby qubits that aren’t also being measured. This is a significant problem for error correcting circuits which all rely on mid-circuit measurements. Broadly speaking, there are two complementary strategies for mitigating measurement induced decoherence. The first is to incorporate techniques that suppress the decoherence, and the second is to move the ions some distance away to be measured safely. Both of these strategies will be discussed in the following subsections.

1. Techniques for suppressing decoherence

One way to limit measurement induced decoherence is to shorten the amount of time the qubit(s) are illuminated. This comes at the cost of measurement fidelity since there are fewer scattered photons to be detected. Naturally, faster and higher fidelity measurements will be possible with improvements in the photon collection rate and photo-detector efficiency. See the introduction of Wolk et. al. for a brief summary of techniques used to improve sparse detection fidelities [30].

Another approach for protecting against decoherence is to use quantum logic spectroscopy [31]. This is when the information of one qubit is transferred onto an ion of a different species that when measured emits off-resonant photons which are unlikely to disturb the states of neighboring qubits. An accidental benefit of this approach is that preexisting cooling ions may be used for this purpose. The disadvantages of quantum logic spectroscopy are that it is more difficult to maintain coherent control of multiple ion-species simultaneously, and that it requires additional ions (at most double for a one-to-one pairing). A promising alternative might be to use ions of the same species but have the data and measurement qubits encoded in different energy levels of the ion [32] [33]. An alternative strategy would be to suppress the decoherence effects altogether so that additional measurement ions are not required. Gaebler et. al. [34] demonstrate a technique for reducing measurement cross-talk errors by an order of magnitude using tailored *micromotion* which may reduce and potentially eliminate the need for

logic spectroscopy or shuttling altogether. Micromotion is a time-dependent, driven motion that naturally occurs as a result of ion confinement. Too much micromotion however is known to push ions outside the *Lamb-Dicke regime*, making high fidelity gates infeasible. Using tailored micromotion to hide ions from fluorescence induced measurements may therefore require more cooling than usual.

2. Ion-shuttling speeds

Perhaps the most intuitive strategy for mitigating measurement induced decoherence is to move the ions a safe distance away before measuring them. Ideally we’d like to complete this operation as fast as possible, but faster shuttling introduces more thermal noise which can have a detrimental effect on two-qubit gates in particular. Broadly speaking, the infidelity of a Mølmer-Sørensen gate (See section III C) applied between two qubits in an ion-chain is known to depend on both the temperature of the chain and its displacement in phase space. These effects have been fully characterised for two different error metrics [35]. In the ion-shuttling literature, the amount of heat imparted in transport is commonly characterised in terms of how much the expected *energy quanta* of a particular motional mode increases. Sterk et. al. [36] use the results of Ruzic et. al. [35] to develop a helpful rule-of-thumb: Trapped-ions in a linear chain can each tolerate around 1 quanta of energy before there is an appreciable drop in the Mølmer-Sørensen gate fidelity. The fastest and quietest reported shuttling operation at the time of writing is also from Sterk et. al. who demonstrate a $210\mu\text{m}$ one way ion transport in $6\mu\text{s}$ with a maximum gain of 0.36 ± 0.08 quanta for an average speed of $35 \mu\text{m } \mu\text{s}^{-1}$ [36]. Slower, but more conservative routing was also demonstrated in $55\mu\text{s}$ with a gain in 0.1 quanta [37].

3. Estimates for shuttling times

How far do ions need to be separated for the effects of measurement induced decoherence to be considered negligible? At the shorter end, Pino et. al. report a QCCD architecture where a shuttling distance of $110\mu\text{m}$ resulted in cross-talk errors between 3.5×10^{-3} and 1.5×10^{-2} [20]. Similarly, Crain et. al. show that a separation of $370\mu\text{m}$ results in cross-talk errors of 2×10^{-5} [28]. If we assume a distance of $300\mu\text{m}$ is tolerable, then with the shuttling speed reported by Sterk et. al. we can assume that a two-way shuttling time of around $10\mu\text{s}$ is sufficient for eliminating decoherence effects.

4. Multi qubit measurements

Strategic multi-qubit fluorescence measurements may be an effective way to reduce shuttling time further since high fidelity measurements are possible on *groups* of proximate ions. Zhukhas et. al. for example present a four ion readout with an overall error lower than twenty parts per million [38]. Similarly, IonQ's *Harmony* device is able to perform an 11 qubit readout with a cross-talk error lower than 10^{-4} [39]. Assuming their linear trap is around 100 micrometers long, this would suggest that ion separations below $10\mu\text{m}$ or so are sufficient for high fidelity simultaneous measurements.

C. Cooling trapped ions

All gates and operations of trapped ion quantum computers require low temperatures, but this is especially true of the two qubit gates since they depend on vibrational coupling which is highly sensitive to noise. In the early days of trapped ion-quantum computing, two qubit gates required temperatures close to the ground state energy. The breakthrough discovery of Mølmer and Sørensen [40] shifted this paradigm by introducing a gate that could operate at the *Doppler temperature* – the temperature regime attainable with *Doppler cooling*. In the following subsections, we present a brief review of the cooling techniques used to bring *collections of ions* to Doppler and sub-Doppler temperatures – endeavoring to report approximate cooling times wherever possible. Although cooling single ions is considerably easier than cooling ion crystals (since there are fewer motional modes to be addressed [41]), it is unlikely that single-ion cooling will be a leading technology in the context of quantum computation. This is because virtually all quantum architectures (with the possible exception of QCCDs) keep their computational ions organised in crystals.

At a high level, Doppler cooling works by shining a laser on an ion with a frequency just below what the ion will absorb. When the ion moves towards the laser, the incoming light is blue-shifted with respect to the ion which causes it to absorb a photon and slow down. Aside from Doppler cooling, other established laser based cooling techniques that operate under similar principles include resolved sideband cooling, Raman sideband cooling, and Electromagnetically Induced Transparency cooling (EIT) with the fastest of these being EIT. Feng et. al. report cooling a 40 ion chain to a near ground state energy in under $300\mu\text{s}$ [42] while Jordan et. al. reach similar temperatures for a 100 ion Penning trap within $200\mu\text{s}$. Some disadvantages of EIT are that it has a limited range of motional frequencies it can cool, and it is slow at cooling low frequency excitations [43].

Sympathetic cooling, where cold ions are brought into physical contact with computational ions, has been discussed in some detail in the previous sections. The major disadvantage of this approach is that it is relatively slow

compared to other cooling methods and requires additional resource overheads [44]. A recent experimental demonstration showed that ion chains up to length 28 could be cooled to the global Doppler cooling limit using only two dedicated cooling ions of the same species [45]. This paper reported *relaxation times* (defined as the time required for the noise to settle within 5% of noise of the initial state) between 10 and 100 ms . Though these numbers are somewhat discouraging, one promising direction for further study is *persistent cooling* where a number of sympathetic cooling ions are brought in perpetual contact with computational ions. As the computation proceeds, the cooling ions are continuously chilled with Doppler cooling. This technique could lift the requirement for cooling processes that halt the computation. Lin et. al. present an analysis of the dynamics of a linear array where a small subset of the ions are continuously cooled [46]. Additionally, a theoretic proposal for sympathetic cooling between one ion and a pre-cooled resource ion can be accomplished on the order of tens of microseconds, which may find some applicability in this context [47].

D. Cycle time paradigms

At the beginning of this section (III), we mentioned that estimating attainable cycle times is crucial to our resource estimation task. This is because the cycle time has a *direct bearing* on the number of communication ions we require per ELU; Faster cycles mean that more ions are required to collect the necessary entanglement in a shorter period. In this section we synthesise our findings from the previous review by proposing three *cycle time paradigms* ($1000\mu\text{s}$, $100\mu\text{s}$, $10\mu\text{s}$) that we could reasonably expect to see achieved for trapped-ion surface codes given various technical assumptions. For a shorthand summary of these paradigms see Table III D. The first and slowest cycle time we propose is around $1000\mu\text{s}$. This is several times faster than what was simulated by Trout et. al. [24] and around three times slower than the architecture proposed by Lekitsch et. al. [26]. This time scale permits some flexibility in routing and cooling options making it especially suitable for segmented-linear trap and QCCD architectures which require extensive use of both. Here, we expect one or more stages of cooling per cycle and shuttling to avoid measurement induced decoherence. The second time proposed is $100\mu\text{s}$. This is a more optimistic regime, being several times faster than the EIT cooling times reported in Section III C. Because of this, we require that fewer than one dedicated round of cooling is made per clock cycle. There is considerably less flexibility permitted for routing or shuttling at this scale. Dedicated zones for multi-qubit measurement (Section III B 4) will likely become significant time and heat savers as will sub-quanta shuttling. Architectures that are likely to be viable in this paradigm include linear-traps, Wigner crystals, and QCCDs. It is likely

Cycle time	System assumptions
1000 μ s	No assumptions made. Cycle time is comparable to theoretic proposals in literature.
100 μ s	Less than one dedicated round of cooling per cycle. EIT cooling with sub-quanta shuttling required. Multi-qubit measurement stages recommended. Will likely incorporate at least one suppression technique discussed in Sec. III B 1.
10 μ s	Virtually no shuttling allowed. Persistent cooling that doesn't pause syndrome extraction cycle is essential. Multiple suppression techniques from Sec. III B 1 will likely be used together. Purification circuits are low-depth with one round of measurement.

TABLE I. A summary of three cycle time paradigms for trapped-ion surface codes and the various technological milestones required for each speed.

as well that at least one strategy for mitigating measurement induced decoherence will be employed (Section III B 1). The final, and most optimistic regime is 10 μ s. At this timescale, our clock cycle matches the two qubit gate times reported in Sec. III A meaning that no processes are allowed which interrupt syndrome extraction. Persistent cooling is an absolute necessity here, as is an architecture that doesn't require any routing or shuttling. Linear traps, Wigner crystals or micro-trap based architectures are the most likely candidates for this regime.

E. Entangling ion pairs

Any modular architecture requires some means of communicating quantum information between the constituent ELUs. A common approach is to establish *maximally entangled pairs* of qubits between dedicated communication qubits to be used for quantum state teleportation. First, an ion is pulsed to create an entangled pair between an internal state of the ion and an emitted photon. Then, photons emitted from two different ELUs are routed together and fused with an polarization resolving Bell measurement that establishes entanglement between the separated ions. The rate at which ion-ion entanglement is established this way depends on the photon scattering rate (the maximum rate that photons can interact with ions), the photon capture rate, and the probability of the fusion operation succeeding. The photon scattering rate (which can be interpreted as an attempt rate) is physically constrained to around 100 MHz, though experimental instances of this today are practically limited to around 1 MHz [48]. The fastest and highest quality ion-ion distribution rate at the time of writing comes from the same paper cited and reports 94% fidelity Bell pairs

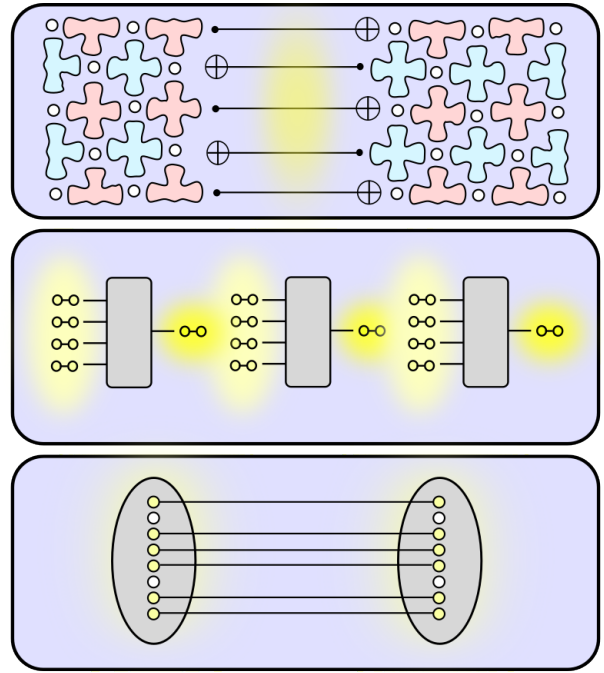


FIG. 3. Three concurrent stages for a single lattice surgery operation. (Bottom) Entanglement is established between pairs of communication ions in separate ELUs. (Middle) Distributed pairs in storage ions are refined via entanglement purification. (Top) Refined pairs are used to teleport the mediating gates needed for a lattice surgery between two surface code patches.

with a success probability of 2.18×10^{-4} for an average pair rate of $182s^{-1}$.

IV. METHODOLOGY

A. A heuristic for fault-tolerant lattice surgery

Our primary objective for this work is to estimate the number of trapped-ions needed to perform *fault-tolerant* lattice surgery between surface codes at the rates specified in Table III D. So far however, we have not addressed the question of what it means for lattice surgery to be fault-tolerant. Here, we formalise a definition by introducing a heuristic consisting of three criteria that must all be met for lattice surgery to be considered fault-tolerant. These conditions correspond to *three subroutines* of lattice surgery, which are depicted in Fig. 4. Essentially, the point of this heuristic is to ensure that each of these necessary subroutines succeeds with high probability.

The first criteria is the promise of a *purification protocol* that takes n Bell pairs of some initial fidelity F_{in} and, with some probability p , returns one pair at or above the required fidelity threshold F_{ideal} . The second condition is that each purification circuit is *multiplexed* (run in parallel copies) until the probability of getting at least one

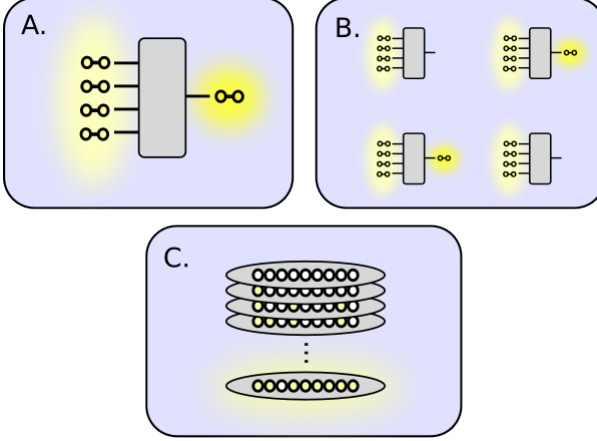


FIG. 4. Illustrations of the three conditions we require for our lattice surgery to be considered fault-tolerant: (A): We are given an $n \rightarrow 1$ purification protocol where the output pair meets or exceeds fidelity F_{ideal} . (B): We duplicate the circuit until the probability of getting at least one purified pair exceeds P_{pair} . (C): We have enough communication ions such that after after a collection time T , we are sure up to a confidence of P_{LS} that we have enough entangled implement D instances of the protocol described in (B).

pair from the lot exceeds P_{pair} . The final condition is that we are able to collect enough entanglement within the cycle time T to implement d instances of the multiplexed purification protocol (one for each “stitch” of the lattice surgery). We stress that this collection *must* take place within the time T so that enough entanglement is acquired to be used for the next round of lattice surgery. The probability that this collection succeeds must equal or exceed a threshold P_{LS} .

1. Minimum number of communication ions required given cycle time

Let p be the success probability of a purification circuit. The probability of obtaining at least one success out of n trials is $1 - (1 - p)^n$. Naturally the minimum number of purification circuits needed to produce at least one pair with a confidence of P_{pair} is then

$$K \equiv \min_n \left[1 - (1 - p)^n \geq P_{\text{pair}} \right] \quad (1)$$

If the purification circuit takes N_p raw pairs as input and returns one pair as output, the total number of raw pairs needed for the lattice surgery according to our heuristic is

$$N_{\text{LS}} = D N_p K \quad (2)$$

If T is the surface code clock cycle (the time it takes to perform a round of syndrome extraction) and if R is the

rate at which entanglement can be attempted between pairs of ions, then we have $A = TR$ attempts to collect N_{LS} pairs. Suppose each ELU has $N_{\text{ions}} > N_{\text{LS}}$ communication ions. During a collection attempt, each of the $v \leq N_{\text{ions}}$ vacant ions are pulsed and may become entangled with probability p_e . Entangled ions are not pulsed in subsequent rounds, and we assume the entanglement does not degrade as it waits. Our first objective is to determine the probability that N_{LS} pairs can be collected in A attempts. The probability that a single ion pair is entangled after A attempts is given by:

$$P_{\text{onepair}} = 1 - (1 - p_e)^A \quad (3)$$

Let $X \sim \mathcal{B}(N_{\text{ions}}, P_{\text{onepair}})$ be the binomial random variable representing the number of ion pairs out of the initial N_{ions} that are populated after A rounds. The minimum number of communication ions needed to collect at least N_{LS} pairs in a code cycle with confidence P_{LS} is then

$$\min_{N_{\text{ions}}} \left[P(X \geq N_{\text{LS}}) \geq P_{\text{LS}} \right] \quad (4)$$

2. Maximum attainable rate given given number of communication ions

Suppose now that N_{ions} is fixed. Let A_{\min} be the minimum number of attempts needed to populate the N_{LS} ions needed for lattice surgery with an overall confidence of P_{LS} .

$$A_{\min} = \min_A \left[P(X \geq D N_p K) \geq P_{\text{LS}} \right] \quad (5)$$

The maximum attainable rate for our fault-tolerant lattice surgery given N_{ions} is then just A_{\min}/R

B. Device parameters and assumptions

From Stephenson et. al. [48], we assume that we can pulse ions at a rate of 1MHz where each pulse has a 2.18×10^{-4} chance of producing an entangled ion-ion pair of fidelity 0.94. We assume that our surface codes have an operational error rate of 0.1% which, from the results of Ramette et. al. [13], means we can tolerate Bell pairs with an infidelity of 0.01. We assume that the routing and circuits within the purification stage take a negligible amount of time compared with the entanglement collection. Single and two qubit gate error are approximated as single and two-qubit depolarizing channels that occur with probabilities 1×10^{-5} and 5×10^{-5} respectively. Measurement errors are taken as bitflip channels that occur with probability 1×10^{-5} . Although ion-trapping

lifetimes are extremely good (hours, and even months in extreme cases), they are not indefinite. We do not consider ion loss or replacement in our resource estimation. Neither do we consider leakage errors that are known to accumulate with consecutive surface code cycles [49]. Though a linear crystal architecture has all-to-all connectivity in theory, it may not be possible in practice to perform arbitrary simultaneous two qubit gates as we have assumed. Nevertheless, we note promising results from the current state-of-the-art [50].

C. Optimizing entanglement purification with device level noise

Our need for fault-tolerant lattice surgery highlights the importance of a high yield pair purification protocol. Though all such protocols theoretically asymptote to unit fidelity, the practical reality is that device level noise imposes a cap on the pair fidelities that are attainable with purification. It is essential therefore to find a purification protocol that is able to reach our target fidelity of $F_{\text{ideal}} = 0.99$ despite circuit-level noise. To this end, we decided to search for high-performing purification protocols using recently developed numerical methods. Goodenough et. al. proposed an exhaustive search over purification protocols by mapping the problem to an enumeration over so called *graph codes* [52], while Addala et. al. [51], built on earlier work from Krastanov et. al. [53] to refine a genetic algorithm for finding purification protocols. We opted to use the genetic optimization over the enumeration because of its ease of use and because the attainable fidelities reported by Addala et. al. were comparable to those reported by Goodenough. We used this genetic algorithm to identify several hundred potentially suitable purification circuits. From this initial pool of candidates, we simulated each circuit using the noise parameters detailed in IV B. For added realism, we modeled our initial $F = 0.94$ entangled pairs after the density matrix of an experimentally realised ion-ion pair reported in the supplementary material of Stephenson et. al. [48] (See appendix). The highest yield purification circuit we discovered with this genetic algorithm is presented in fig. 5. This protocol takes three *Stephenson pairs* as input and produces one output pair with a fidelity of $F = 0.9904$ with an overall success probability of 0.819. A full discussion of our methodology and findings is presented in the appendix of this paper.

V. RESULTS

Our numerical results are presented as tables in Fig. 6 and Fig. 7 respectively. In Fig. 6 we used Eq. 4 to determine the minimum number of communication ions needed to collect sufficiently many entangled pairs for fault-tolerant lattice surgery for a given cycle time T . We considered three cycle times of $10\mu\text{s}$, $100\mu\text{s}$, and $1000\mu\text{s}$

according to the technological paradigms we discussed in section III over a small range of code distances. Our calculations indicate that the number of communication ions required is approximately linear with respect to both the code distance and the cycle time within our selected ranges. As the cycle time decreases in orders of magnitude, we find straightforwardly that the number of communication ions increases in orders of magnitude. If we assume that a given ELU may contain around 1000 ions at most, we find that a $D = 9$ code is theoretically supported at a clock cycle $1000\mu\text{s}$, while cycle times considerably faster than this appear out of reach.

In fig 7, we used Eq. 5 to calculate the maximum lattice surgery rates that are theoretically possible according to our fault-tolerant heuristic given various numbers of communication ions and various code distances. The white squares in the 100 ion column from $D = 7$ onward indicate that fault-tolerant lattice surgery is not possible at these distances, since the number of required pairs exceeds the number of communication ions available. Similar to what we observed in the previous table, we find that there's a tenfold difference between the 1,000 and 10,000 ion columns, though we note a slight deviation from this trend at the 100 ion column. This behavior occurs because the number of communication ions is close to the number of required pairs. As the required number of pairs approaches the number of available ions, we expect an exponential increase in the number of attempts needed to collect the entanglement since this collection is done without replacement. Our results indicate that with 100 communication ions, we could expect to support a distance 5 or 6 code at a maximum rate of around 100Hz. For 1000 and 10000 communication ions we find that larger code distances are possible with rates at around 1KHz and 10KHz respectively.

VI. DISCUSSION

Our results, although promising for short term demonstrations of surface code quantum computing, indicate long term concerns for scalability due to the large number of physical resources required. If $10\mu\text{s}$ is about the fastest clock cycle we can hope for, our findings in figure 6 indicate that we would need upwards of 40,000 communication ions per ELU even for modestly sized surface codes. The prohibitive cost of this indicates an urgent need for improved optical coupling; As it stands, the low probability of entangling ions in separate ELUs (2.18×10^{-4} [48]) is a leading cause for this inflated resource overhead. Though ion-photon interaction rates appear to be limited by physical constraints, we anticipate that improvements can be made in photon collection rates. Literature today reports photon collection efficiencies as high as 10% – roughly an order of magnitude above what was previously possible [54]. Entanglement distribution using neutral atoms to mediate interactions has been discussed in the context of quantum network-

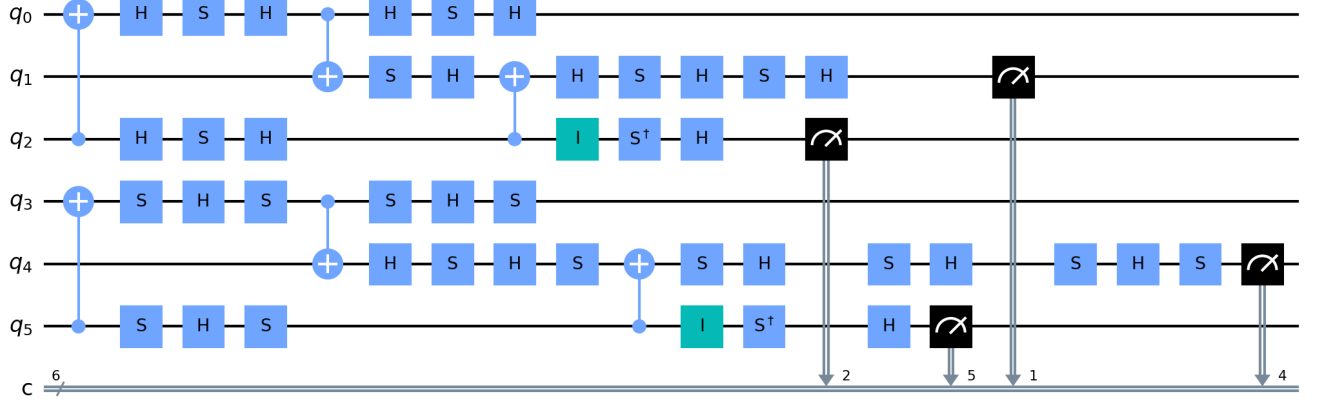


FIG. 5. A high yield purification circuit discovered by the genetic algorithm from Addala et. al. [51]. This circuit takes three partially entangled pairs as input $\{(q_0, q_3), (q_1, q_3), (q_2, q_5)\}$ and non-deterministically returns a higher fidelity pair at (q_0, q_3) . The protocol succeeds if $c_1 = c_4$ and $c_2 \neq c_5$ (in other words, the measurement outcome of qubit q_1 is coincident with the measurement of q_4 and the measurement of q_2 is anti-coincident with q_5). When this circuit is run with three copies of the *Stephenson pair* (see Appendix) as input together with the noise parameters described in sec. IV B, the purification produces a fidelity $F = 0.9904$ pair with probability $p = 0.819$

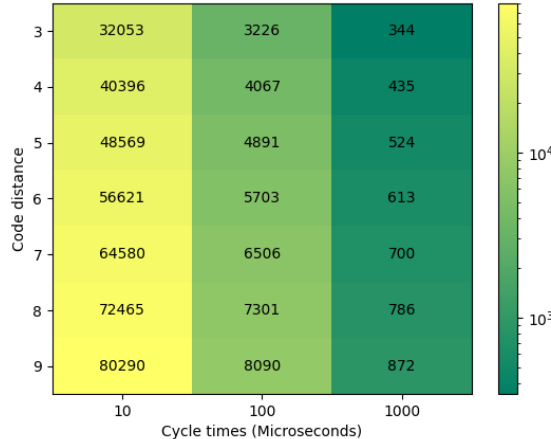


FIG. 6. Minimum numbers of communication ions required to ensure that sufficient entanglement can be collected. Minimum number of communication ions required to ensure that sufficient entanglement can be enough entanglement can be supplied within a given cycle time.

ing [55]. We note as well that our purification protocol is another target for improvement. Our $3 \rightarrow 1$ protocol has a 81.9% success rate, which for a confidence threshold of $P_{\text{Pair}} = 0.999$ means that we require $K = 5$ purification circuits (Eq. 1) per stitch in the lattice surgery. This is effectively a $15 \rightarrow 1$ purification circuit, which appears rather wasteful. It is possible that further developments in the study of entanglement purification will result in high-confidence protocols with higher overall yield.

In this work we estimated the number of communica-

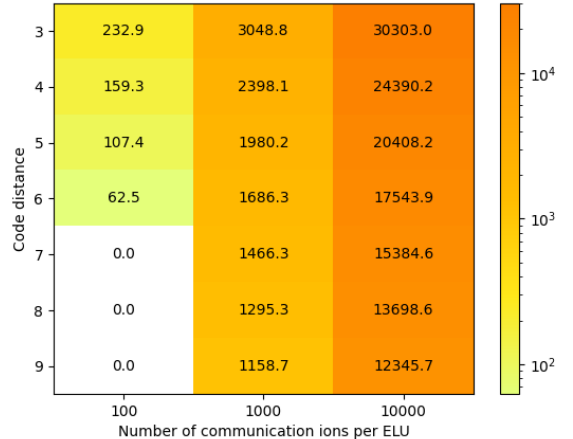


FIG. 7. Average lattice surgery rates for different code distances and numbers of communication ions

tion ions needed to perform lattice surgery between two trapped-ion surface code qubits. To this end, we developed three paradigms for syndrome extraction cycle times that were predicated on various technological milestones and presented a heuristic for determining whether a lattice surgery operation is fault tolerant.

VII. ACKNOWLEDGEMENT AND FUNDING

We thank Ilia Khait, Stefan Krastanov, Vaishnavi Addala, and Kenneth Goodenough for helpful discussions. The views, opinions, and/or findings expressed are those

of the author(s) and should not be interpreted as representing the official views or policies of the Department of Defense or the U.S. Government. This research was developed with funding from the Defense Advanced Research Projects Agency [under the Quantum Benchmarking (QB) program under Awards No. HR00112230007

and No. HR001121S0026 contracts].

A.M.D.G

[1] Colin D. Bruzewicz, John Chiaverini, Robert McConnell, and Jeremy M. Sage. Trapped-ion quantum computing: Progress and challenges. *Applied Physics Reviews*, 6(2):021314, Jun 2019. ISSN 1931-9401. doi: 10.1063/1.5088164. URL <http://dx.doi.org/10.1063/1.5088164>.

[2] Bjoern Lekitsch, Sebastian Weidt, Austin G. Fowler, Klaus Mølmer, Simon J. Devitt, Christof Wunderlich, and Winfried K. Hensinger. Blueprint for a microwave trapped ion quantum computer. *Science Advances*, 3 (2):e1601540, 2017. doi:10.1126/sciadv.1601540. URL <https://www.science.org/doi/abs/10.1126/sciadv.1601540>.

[3] Kae Nemoto, Michael Trupke, Simon J. Devitt, Ashley M. Stephens, Burkhard Scharfenberger, Kathrin Buczak, Tobias Nöbauer, Mark S. Everitt, Jörg Schmiedmayer, and William J. Munro. Photonic architecture for scalable quantum information processing in diamond. *Phys. Rev. X*, 4:031022, Aug 2014. doi: 10.1103/PhysRevX.4.031022. URL <https://link.aps.org/doi/10.1103/PhysRevX.4.031022>.

[4] Joschka Roffe. Quantum error correction: an introductory guide. *Contemporary Physics*, 60(3):226–245, 2019.

[5] Kevin S. Chou, Jacob Z. Blumoff, Christopher S. Wang, Philip C. Reinhold, Christopher J. Axline, Yvonne Y. Gao, L. Frunzio, M. H. Devoret, Liang Jiang, and R. J. Schoelkopf. Deterministic teleportation of a quantum gate between two logical qubits. *Nature*, 561 (7723):368–373, September 2018. ISSN 1476-4687. doi: 10.1038/s41586-018-0470-y. URL <http://dx.doi.org/10.1038/s41586-018-0470-y>.

[6] Charles H. Bennett, Gilles Brassard, Sandu Popescu, Benjamin Schumacher, John A. Smolin, and William K. Wootters. Purification of noisy entanglement and faithful teleportation via noisy channels. *Physical Review Letters*, 76(5):722–725, jan 1996. doi:10.1103/physrevlett.76.722.

[7] Austin G. Fowler, Matteo Mariantoni, John M. Martinis, and Andrew N. Cleland. Surface codes: Towards practical large-scale quantum computation. *Physical Review A*, 86(3), Sep 2012. ISSN 1094-1622. doi: 10.1103/physreva.86.032324. URL <http://dx.doi.org/10.1103/PhysRevA.86.032324>.

[8] Ashley M. Stephens. Fault-tolerant thresholds for quantum error correction with the surface code. *Phys. Rev. A*, 89:022321, Feb 2014. doi:10.1103/PhysRevA.89.022321. URL <https://link.aps.org/doi/10.1103/PhysRevA.89.022321>.

[9] David K. Tuckett, Stephen D. Bartlett, and Steven T. Flammia. Ultrahigh error threshold for surface codes with biased noise. *Phys. Rev. Lett.*, 120:050505, Jan 2018. doi:10.1103/PhysRevLett.120.050505. URL <https://link.aps.org/doi/10.1103/PhysRevLett.120.050505>.

[10] Daniel Litinski. A game of surface codes: Large-scale quantum computing with lattice surgery. *Quantum*, 3: 128, March 2019. ISSN 2521-327X. doi:10.22331/q-2019-03-05-128. URL <http://dx.doi.org/10.22331/q-2019-03-05-128>.

[11] Michael Vasmer and Dan E. Browne. Three-dimensional surface codes: Transversal gates and fault-tolerant architectures. *Phys. Rev. A*, 100:012312, Jul 2019. doi: 10.1103/PhysRevA.100.012312. URL <https://link.aps.org/doi/10.1103/PhysRevA.100.012312>.

[12] Clare Horsman, Austin G. Fowler, Simon Devitt, and Rodney Van Meter. Surface code quantum computing by lattice surgery. *New Journal of Physics*, 14(12):123011, dec 2012. doi:10.1088/1367-2630/14/12/123011. URL <https://doi.org/10.1088%2F1367-2630%2F14%2F12%2F123011>.

[13] Joshua Ramette, Josiah Sinclair, Nikolas P. Breuckmann, and Vladan Vuletić. Fault-tolerant connection of error-corrected qubits with noisy links, 2023.

[14] C. Monroe, R. Raussendorf, A. Ruthven, K. R. Brown, P. Maunz, L.-M. Duan, and J. Kim. Large-scale modular quantum-computer architecture with atomic memory and photonic interconnects. *Phys. Rev. A*, 89:022317, Feb 2014. doi:10.1103/PhysRevA.89.022317. URL <https://link.aps.org/doi/10.1103/PhysRevA.89.022317>.

[15] Jwo-Sy Chen, Erik Nielsen, Matthew Ebert, Volkan Inlek, Kenneth Wright, Vandiver Chaplin, Andrii Maksymov, Eduardo Páez, Amrit Poudel, Peter Maunz, and John Gamble. Benchmarking a trapped-ion quantum computer with 29 algorithmic qubits, 2023.

[16] Prakash Murali, Dripto M. Debroy, Kenneth R. Brown, and Margaret Martonosi. Architecting noisy intermediate-scale trapped ion quantum computers. In *Proceedings of the ACM/IEEE 47th Annual International Symposium on Computer Architecture*, ISCA '20, page 529–542. IEEE Press, 2020. ISBN 9781728146614. doi:10.1109/ISCA45697.2020.00051. URL <https://doi-org.ezproxy.lib.uts.edu.au/10.1109/ISCA45697.2020.00051>.

[17] Alexander K. Ratcliffe, Richard L. Taylor, Joseph J. Hope, and André R. R. Carvalho. Scaling trapped ion quantum computers using fast gates and micro-traps. *Phys. Rev. Lett.*, 120:220501, May 2018. doi: 10.1103/PhysRevLett.120.220501. URL <https://link.aps.org/doi/10.1103/PhysRevLett.120.220501>.

[18] Zain Mehdi, Alexander K. Ratcliffe, and Joseph J. Hope. Scalable quantum computation with fast gates in two-dimensional microtrap arrays of trapped ions. *Phys. Rev. A*, 102:012618, Jul 2020. doi: 10.1103/PhysRevA.102.012618. URL <https://link.aps.org/doi/10.1103/PhysRevA.102.012618>.

[19] V. Kaushal, B. Lekitsch, A. Stahl, J. Hilder, D. Pijn, C. Schmiegelow, A. Bermudez, M. Müller, F. Schmidtkaler, and U. Poschinger. Shuttling-based trapped-

ion quantum information processing. *AVS Quantum Science*, 2(1):014101, 03 2020. ISSN 2639-0213. doi: 10.1116/1.5126186. URL <https://doi.org/10.1116/1.5126186>.

[20] J. M. Pino, J. M. Dreiling, C. Figgatt, J. P. Gaebler, S. A. Moses, M. S. Allman, C. H. Baldwin, M. Foss-Feig, D. Hayes, K. Mayer, C. Ryan-Anderson, and B. Neyenhuis. Demonstration of the trapped-ion quantum ccd computer architecture. *Nature*, 592(7853):209–213, April 2021. ISSN 1476-4687. doi: 10.1038/s41586-021-03318-4. URL <http://dx.doi.org/10.1038/s41586-021-03318-4>.

[21] Y.-K. Wu, Z.-D. Liu, W.-D. Zhao, and L.-M. Duan. High-fidelity entangling gates in a three-dimensional ion crystal under micromotion. *Phys. Rev. A*, 103:022419, Feb 2021. doi:10.1103/PhysRevA.103.022419. URL <https://link.aps.org/doi/10.1103/PhysRevA.103.022419>.

[22] S.-T. Wang, C. Shen, and L.-M. Duan. Quantum computation under micromotion in a planar ion crystal. *Scientific Reports*, 5(1), February 2015. ISSN 2045-2322. doi: 10.1038/srep08555. URL <http://dx.doi.org/10.1038/srep08555>.

[23] Tyler Leblond, Ryan S. Bennink, Justin G. Lietz, and Christopher M. Seck. Tisc: A surface code compiler and resource estimator for trapped-ion processors. SC-W '23, page 1426–1435, New York, NY, USA, 2023. Association for Computing Machinery. ISBN 9798400707858. doi:10.1145/3624062.3624214. URL <https://doi.org/10.1145/3624062.3624214>.

[24] Colin J Trout, Muyuan Li, Mauricio Gutiérrez, Yukai Wu, Sheng-Tao Wang, Luming Duan, and Kenneth R Brown. Simulating the performance of a distance-3 surface code in a linear ion trap. *New Journal of Physics*, 20(4):043038, April 2018. ISSN 1367-2630. doi: 10.1088/1367-2630/aab341. URL <http://dx.doi.org/10.1088/1367-2630/aab341>.

[25] Ying Li and Simon C. Benjamin. One-dimensional quantum computing with a ‘segmented chain’ is feasible with today’s gate fidelities. *npj Quantum Information*, 4(1), May 2018. ISSN 2056-6387. doi: 10.1038/s41534-018-0074-2. URL <http://dx.doi.org/10.1038/s41534-018-0074-2>.

[26] Bjoern Lekitsch, Sebastian Weidt, Austin G. Fowler, Klaus Mølmer, Simon J. Devitt, Christof Wunderlich, and Winfried K. Hensinger. Blueprint for a microwave trapped ion quantum computer. *Science Advances*, 3(2):e1601540, 2017. doi:10.1126/sciadv.1601540. URL <https://www.science.org/doi/abs/10.1126/sciadv.1601540>.

[27] Colin D. Bruzewicz, John Chiaverini, Robert McConnell, and Jeremy M. Sage. Trapped-ion quantum computing: Progress and challenges. *Applied Physics Reviews*, 6(2): 021314, 05 2019. ISSN 1931-9401. doi:10.1063/1.5088164. URL <https://doi.org/10.1063/1.5088164>.

[28] Stephen Crain, Clinton Cahall, Geert Vrijen, Emma E. Wollman, Matthew D. Shaw, Varun B. Verma, Sae Woo Nam, and Jungsang Kim. High-speed low-crosstalk detection of a 171yb+ qubit using superconducting nanowire single photon detectors. *Communications Physics*, 2(1), August 2019. ISSN 2399-3650. doi: 10.1038/s42005-019-0195-8. URL <http://dx.doi.org/10.1038/s42005-019-0195-8>.

[29] A. H. Myerson, D. J. Szwarc, S. C. Webster, D. T. C. Allcock, M. J. Curtis, G. Imreh, J. A. Sherman, D. N. Stacey, A. M. Steane, and D. M. Lucas. High-fidelity readout of trapped-ion qubits. *Phys. Rev. Lett.*, 100:200502, May 2008. doi: 10.1103/PhysRevLett.100.200502. URL <https://link.aps.org/doi/10.1103/PhysRevLett.100.200502>.

[30] Sabine Wolk, Ch Piltz, Theeraphot Sriarunothai, and Christof Wunderlich. State selective detection of hyperfine qubits. *Journal of Physics B: Atomic*, 48, 04 2015. doi:10.1088/0953-4075/48/7/075101.

[31] P. O. Schmidt, T. Rosenband, C. Langer, W. M. Itano, and et al. Spectroscopy using quantum logic. *Science*, 309(5735):749–52, Jul 29 2005. URL <http://ezproxy.lib.uts.edu.au/login?url=https://www.proquest.com/scholarly-journals/spectroscopy-using-quantum-logic/docview/213616639/se-2>. Copyright - Copyright American Association for the Advancement of Science Jul 29, 2005; Document feature - Equations; Diagrams; Graphs; ; Last updated - 2023-12-04; CODEN - SCIEAS.

[32] L. Feng, Y. Y. Huang, Y. K. Wu, W. X. Guo, J. Y. Ma, H. X. Yang, L. Zhang, Y. Wang, C. X. Huang, C. Zhang, L. Yao, B. X. Qi, Y. F. Pu, Z. C. Zhou, and L. M. Duan. Realization of a crosstalk-avoided quantum network node with dual-type qubits by the same ion species, 2023.

[33] H.-X. Yang, J.-Y. Ma, Y.-K. Wu, Y. Wang, M.-M. Cao, W.-X. Guo, Y.-Y. Huang, L. Feng, Z.-C. Zhou, and L.-M. Duan. Realizing coherently convertible dual-type qubits with the same ion species. *Nature Physics*, 18(9):1058–1061, August 2022. ISSN 1745-2481. doi: 10.1038/s41567-022-01661-5. URL <http://dx.doi.org/10.1038/s41567-022-01661-5>.

[34] J. P. Gaebler, C. H. Baldwin, S. A. Moses, J. M. Dreiling, C. Figgatt, M. Foss-Feig, D. Hayes, and J. M. Pino. Suppression of midcircuit measurement crosstalk errors with micromotion. *Phys. Rev. A*, 104:062440, Dec 2021. doi:10.1103/PhysRevA.104.062440. URL <https://link.aps.org/doi/10.1103/PhysRevA.104.062440>.

[35] B. P. Ruzic, T. A. Barrick, J. D. Hunker, R. J. Law, B. K. McFarland, H. J. McGuinness, L. P. Parazzoli, J. D. Sterk, J. W. Van Der Wall, and D. Stick. Entangling-gate error from coherently displaced motional modes of trapped ions. *Phys. Rev. A*, 105:052409, May 2022. doi:10.1103/PhysRevA.105.052409. URL <https://link.aps.org/doi/10.1103/PhysRevA.105.052409>.

[36] Jonathan D. Sterk, Henry Coakley, Joshua Goldberg, Vincent Hietala, Jason Lechtenberg, Hayden McGuinness, Daniel McMurtrey, L. Paul Parazzoli, Jay Van Der Wall, and Daniel Stick. Closed-loop optimization of fast trapped-ion shuttling with sub-quanta excitation. *npj Quantum Information*, 8(1):68, Jun 2022. ISSN 2056-6387. doi:10.1038/s41534-022-00579-3. URL <https://doi.org/10.1038/s41534-022-00579-3>.

[37] R. Bowler, J. Gaebler, Y. Lin, T. R. Tan, D. Hanneke, J. D. Jost, J. P. Home, D. Leibfried, and D. J. Wineland. Coherent diabatic ion transport and separation in a multizone trap array. *Phys. Rev. Lett.*, 109:080502, Aug 2012. doi:10.1103/PhysRevLett.109.080502. URL <https://link.aps.org/doi/10.1103/PhysRevLett.109.080502>.

[38] Liudmila A. Zhukas, Peter Svihra, Andrei Nomerotski, and Boris B. Blinov. High-fidelity simultaneous detection of a trapped-ion qubit register. *Phys. Rev. A*, 103: 062614, Jun 2021. doi:10.1103/PhysRevA.103.062614. URL <https://link.aps.org/doi/10.1103/PhysRevA.103.062614>.

[39] K. Wright, K. M. Beck, S. Debnath, J. M. Amini, Y. Nam, N. Grzesiak, Chen J-S, N. C. Pisenti, M. Chmielewski, C. Collins, K. M. Hudek, J. Mizrahi, J. Wong-Campos, S. Allen, J. Apisdorf, P. Solomon, M. Williams, A. M. Ducore, A. Blinov, S. M. Kreikemeier, V. Chaplin, M. Keesan, C. Monroe, and J. Kim. Benchmarking an 11-qubit quantum computer. *Nature Communications*, 10:1–6, 11 2019. URL <http://ezproxy.lib.uts.edu.au/login?url=https://www.proquest.com/scholarly-journals/benchmarking-11-qubit-quantum-computer/docview/2319732029/se-2>.

[40] Anders Sørensen and Klaus Mølmer. Quantum computation with ions in thermal motion. *Phys. Rev. Lett.*, 82:1971–1974, Mar 1999. doi:10.1103/PhysRevLett.82.1971. URL <https://link.aps.org/doi/10.1103/PhysRevLett.82.1971>.

[41] Mingyu Kang, Qiyao Liang, Ming Li, and Yunseong Nam. Efficient motional-mode characterization for high-fidelity trapped-ion quantum computing. *Quantum Science and Technology*, 8(2):024002, jan 2023. doi:10.1088/2058-9565/acb3f1. URL <https://dx.doi.org/10.1088/2058-9565/acb3f1>.

[42] L. Feng, W. L. Tan, A. De, A. Menon, A. Chu, G. Pagano, and C. Monroe. Efficient ground-state cooling of large trapped-ion chains with an electromagnetically-induced-transparency tripod scheme. *Phys. Rev. Lett.*, 125:053001, Jul 2020. doi:10.1103/PhysRevLett.125.053001. URL <https://link.aps.org/doi/10.1103/PhysRevLett.125.053001>.

[43] M K Joshi, A Fabre, C Maier, T Brydges, D Kiesenhofer, H Hainzer, R Blatt, and C F Roos. Polarization-gradient cooling of 1d and 2d ion coulomb crystals. *New Journal of Physics*, 22(10):103013, October 2020. ISSN 1367-2630. doi:10.1088/1367-2630/abb912. URL <https://dx.doi.org/10.1088/1367-2630/abb912>.

[44] Y. Lin, J. P. Gaebler, T. R. Tan, R. Bowler, J. D. Jost, D. Leibfried, and D. J. Wineland. Sympathetic electromagnetically-induced-transparency laser cooling of motional modes in an ion chain. *Phys. Rev. Lett.*, 110:153002, Apr 2013. doi:10.1103/PhysRevLett.110.153002. URL <https://link.aps.org/doi/10.1103/PhysRevLett.110.153002>.

[45] Z.-C. Mao, Y.-Z. Xu, Q.-X. Mei, W.-D. Zhao, Y. Jiang, Y. Wang, X.-Y. Chang, L. He, L. Yao, Z.-C. Zhou, Y.-K. Wu, and L.-M. Duan. Experimental realization of multi-ion sympathetic cooling on a trapped ion crystal. *Phys. Rev. Lett.*, 127:143201, Sep 2021. doi:10.1103/PhysRevLett.127.143201. URL <https://link.aps.org/doi/10.1103/PhysRevLett.127.143201>.

[46] Guin-Dar Lin and L.-M. Duan. Sympathetic cooling in a large ion crystal. *Quantum Information Processing*, 15(12):5299–5313, November 2015. ISSN 1573-1332. doi:10.1007/s11128-015-1161-3. URL <https://dx.doi.org/10.1007/s11128-015-1161-3>.

[47] T. Sägesser, R. Matt, R. Oswald, and J. P. Home. Robust dynamical exchange cooling with trapped ions. *New Journal of Physics*, 22(7):073069, July 2020. ISSN 1367-2630. doi:10.1088/1367-2630/ab9e32. URL <https://doi.org/10.1088/1367-2630/ab9e32>.

[48] L. J. Stephenson, D. P. Nadlinger, B. C. Nichol, S. An, P. Drmota, T. G. Ballance, K. Thirumalai, J. F. Goodwin, D. M. Lucas, and C. J. Ballance. High-rate, high-fidelity entanglement of qubits across an elementary quantum network. *Phys. Rev. Lett.*, 124:110501, Mar 2020. doi:10.1103/PhysRevLett.124.110501. URL <https://link.aps.org/doi/10.1103/PhysRevLett.124.110501>.

[49] Natalie C. Brown and Kenneth R. Brown. Leakage mitigation for quantum error correction using a mixed qubit scheme. *Phys. Rev. A*, 100:032325, Sep 2019. doi:10.1103/PhysRevA.100.032325. URL <https://link.aps.org/doi/10.1103/PhysRevA.100.032325>.

[50] Nikodem Grzesiak, Reinhold Blümel, Kenneth Wright, Kristin M. Beck, Neal C. Pisenti, Ming Li, Vandiver Chaplin, Jason M. Amini, Shantanu Debnath, Jwo-Sy Chen, and Yunseong Nam. Efficient arbitrary simultaneously entangling gates on a trapped-ion quantum computer. *Nature Communications*, 11(1), June 2020. ISSN 2041-1723. doi:10.1038/s41467-020-16790-9. URL <https://dx.doi.org/10.1038/s41467-020-16790-9>.

[51] Vaishnavi L. Addala, Shu Ge, and Stefan Krastanov. Faster-than-clifford simulations of entanglement purification circuits and their full-stack optimization, 2023.

[52] Kenneth Goodenough, Sébastien de Bone, Vaishnavi L. Addala, Stefan Krastanov, Sarah Jansen, Dion Gijswijt, and David Elkouss. Near-term n to k distillation protocols using graph codes, 2023.

[53] Stefan Krastanov, Victor V. Albert, and Liang Jiang. Optimized Entanglement Purification. *Quantum*, 3:123, February 2019. ISSN 2521-327X. doi:10.22331/q-2019-02-18-123. URL <https://doi.org/10.22331/q-2019-02-18-123>.

[54] Allison L. Carter, Jameson O'Reilly, George Toh, Sagnik Saha, Mikhail Shalaev, Isabella Goetting, and Christopher Monroe. Ion Trap with In-Vacuum High Numerical Aperture Imaging for a Dual-Species Modular Quantum Computer. *arXiv e-prints*, art. arXiv:2310.07058, October 2023. doi:10.48550/arXiv.2310.07058.

[55] John Hannegan, James D. Sivers, Jake Cassell, and Qudsia Quraishi. Improving entanglement generation rates in trapped-ion quantum networks using nondestructive photon measurement and storage. *Phys. Rev. A*, 103:052433, May 2021. doi:10.1103/PhysRevA.103.052433. URL <https://link.aps.org/doi/10.1103/PhysRevA.103.052433>.

Appendix: Noisy entanglement distillation

Implementations $\tilde{\mathcal{D}}$ of any entanglement distillation protocol \mathcal{D} are generally subjected to noise in the sense that $0 \neq \|\tilde{\mathcal{D}} - \mathcal{D}\| \leq \epsilon$ for small ϵ . Here we benchmark the performance of entanglement distillation protocols obtained with genetic algorithm [51] subjected to noise in ion trap systems. The genetic algorithm takes a Bell-diagonal state

$$F\phi_+ + (1-F)(p_x\psi_+ + p_z\phi_- + p_y\psi_-)$$

as input and searches for optimal $n \rightarrow k$ purification protocols for that state by iterating an initial randomly generated population of circuits (describing entanglement distillation protocols) over a number of generations. The fitness of the individuals in the population is evaluated with respect to one of several possible objective functions.

We optimized with respect to the “average marginal fidelity,” which is the average fidelity of each output pair traced out from the final ensemble. This is determined analytically and may optionally account for single and two qubit depolarizing gate noise along with measurement errors. Each output circuit is returned with its average marginal fidelity and overall success probability.

Although the Bell-diagonal states may at first appear to be a somewhat contrived category of entangled pairs, it turns out that all two-qubit mixed states can be deterministically *twirled* into Bell-diagonal pairs of the same fidelity using local operations and classical communications. This may however cost a small amount of the *distillable entanglement* depending on the input state, though quantifying the amount of entanglement lost and developing recovery techniques appear to be open research directions. For this reason, and because twirling introduces a small amount of noise, we developed our search methodology around the objective of finding purification protocols that could work without twirling.

Our strategy therefore was to perform an initial search for promising looking protocols using $F = 0.94$ Bell-diagonal pairs with $p_x = p_y = p_z = 1/3$ under the parameter values $n = (3, 4, 5)$ and $k = 1$. Our decision to limit our search to $k = 1$ was motivated by our analysis indicating that the $k > 1$ protocols produced output pairs with some amount of *mutual entanglement* between them. This is a significant issue for lattice surgery, since it is assumed that each input pair is independent and required us to restrict ourselves to the $k = 1$ case. Simulating beyond $n = 5$ proved to be unnecessary since the average success rate of the protocols can be seen to decrease with increasing n in Fig. 8. For an $(n > 4) \rightarrow 1$ protocol to have a *higher yield* than the $3 \rightarrow 1$ we identified, it would be necessary for the larger purification circuit to have a significantly higher success probability.

Each simulation was performed with a population of 100 circuits evolved for 150 generations. We selected the top performing circuits from each simulation and benchmarked their performance under the same circuit level noise when simulated with $F = 0.94$ *Stephenson pairs* (See sec. IV C) as input. Our numerical results are presented in Fig. 8. The broad trend indicates that as the number of pairs increases, the success probability of the protocol decreases while the average success probability increases. None of the protocols we identified were able to exceed the required fidelity threshold of $F_{\text{req}} = 0.999$.

Appendix: The Stephenson pair

In section IV C, we alluded to an experimentally realised inter-trap ion pair reported by Stephenson et. al. in the supplementary material of their main paper [48]. Strictly speaking, there are *four pairs* reported which correspond to four possible interferometer detection events. Since these state are all effectively equivalent under local operations and classical communications, we arbitrarily

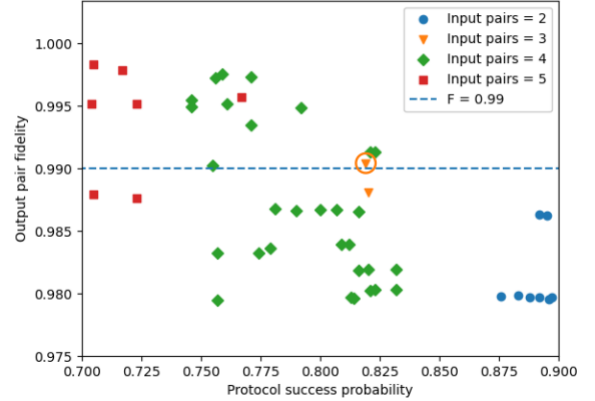


FIG. 8. A scatter plot of the success probabilities and output pair fidelities of a high performing subset of $n \rightarrow 1$ purification protocols that were first identified with the genetic algorithm [51] then simulated under circuit level noise with $F = 0.94$ Stephenson pairs (See eq. A.2) as inputs. The highest yield purification protocol that exceeds the required fidelity threshold $F_{\text{ideal}} = 0.99$ is circled in orange. This is a $3 \rightarrow 1$ purification protocol whose circuit is presented in fig. 5.

chose to consider the state presented in equation A.1. When expressed in the Bell basis, the predominant term of this state is seen to be $|\phi^-\rangle\langle\psi^-|$ up to some phase. As a matter of convenience, it is preferable for this state to be predominantly entangled with respect to $|\phi^+\rangle\langle\phi^+|$. We therefore apply the rotation $(I \otimes XZ)\rho(I \otimes XZ)$ to obtain ρ' in equation A.2. This is the *Stephenson pair* that we refer to in the main body of our paper.

Appendix: Tables of constants

In this section we present two tables that detail the most important free parameters and physical constants used throughout the paper. Table is a summary of the free parameters used and table is a summary of the constants.

$$\rho = \begin{pmatrix} 0.01 & -0.00487616 + 0.00349614i & 0.0135924 + 0.00634402i & 0.00374015 - 0.00331833i \\ -0.00487616 - 0.00349614i & 0.569 & 0.0542638 + 0.440672i & -0.012985 - 0.0292471i \\ 0.0135924 - 0.00634402i & 0.0542638 - 0.440672i & 0.416 & -0.0225074 - 0.00473484i \\ 0.00374015 + 0.00331833i & -0.012985 + 0.0292471i & -0.0225074 + 0.00473484i & 0.005 \end{pmatrix} \quad (\text{A.1})$$

FIG. 9. The “unrotated” Stephenson state, taken from Fig. S4(i) of the supplementary material of [48].

$$\rho' = \begin{pmatrix} 0.569 + 0.i & -0.00487616 - 0.00349614i & -0.0292471 + 0.012985i & 0.440672 - 0.0542638i \\ -0.00487616 + 0.00349614i & 0.01 + 0.i & -0.00331833 - 0.00374015i & 0.00634402 - 0.0135924i \\ -0.0292471 - 0.012985i & -0.00331833 + 0.00374015i & 0.005 + 0.i & -0.0225074 + 0.00473484i \\ 0.440672 + 0.0542638i & 0.00634402 + 0.0135924i & -0.0225074 - 0.00473484i & 0.416 + 0.i \end{pmatrix} \quad (\text{A.2})$$

FIG. 10. A rotated version of Eq. A.1 obtained with the transformation $\rho' = (I \otimes XZ) \rho (I \otimes XZ)$

Parameter	Definition
N_{ions}	The number of communication ions in an ELU
d	Code distance
T	Syndrome extraction cycle time

TABLE II. A summary of the free parameters considered in our analysis.

Parameter	Definition	Value	Justification
p	Purification protocol success probability	0.819	Simulated numerically under circuit level noise
R	Pulse rate	1 MHz	Within the magnitude of what is physically possible [48]
p_c	The probability of entangling two ions with one pulse-attempt	2.18×10^{-4}	State of the art: [48]
F_{ideal}	The fidelity required for pairs used in lattice surgery	0.99	Originally 0.999, but improved thanks to [13]
N_p	The number of pairs required for the purification circuit	3	Fig. 5
P_{pair}	The required confidence for multiplexed purification circuits to produce at least one pair	0.999	Arbitrarily high
K	The required number of purification circuits needed to meet multiplexing confidence	5	Substituting appropriate values into eq. 1
P_{LS}	The required confidence for collecting sufficient entanglement within a given clock cycle	0.999	Arbitrarily high

TABLE III. A catalogue of important numerical constants used throughout this paper with justifications.